ELSEVIER

Biochimica et Biophysica Acta 1466 (2000) 289–305

BIOCHIMICA ET BIOPHYSICA ACTA
BBA

www.elsevier.com/locate/bba

Characterisation of three novel cationic lipids as liposomal complexes with DNA[1]

Marappan Subramanian [a,2], Juha M. Holopainen [a], Tommi Paukku [a], Ove Eriksson [a], Ilpo Huhtaniemi [b], Paavo K.J. Kinnunen [a,*]

[a] *Helsinki Biomembrane and Biophysics Group, Department of Medical Chemistry, Institute of Biomedicine, University of Helsinki, P.O. Box 8, Siltavuorenpenger 10A, 00014 Helsinki, Finland*

[b] *Department of Physiology, Institute of Biomedicine, University of Turku, Kiinamyllynkatu 10, 20520 Turku, Finland*

Received 1 November 1999; received in revised form 14 February 2000; accepted 2 March 2000

Abstract

Cationic lipids (CLs) are being increasingly exploited as transfection vectors for the delivery of DNA into eukaryotic cells. To obtain further insight to the complex formation and interactions between cationic liposomes and DNA, we characterised three novel cationic lipids, viz. bis[2-(11-phenoxyundecanoate)ethyl]-dimethylammonium bromide, *N*-hexadecyl-*N*-{10-[*O*-(4-acetoxy)-phenylundecanoate]ethyl}dimethylammonium bromide, and bis[2-(11-butyloxyundecanoate)ethyl]dimethylammonium bromide. These lipids bear the same charged headgroup yet have different hydrophobic parts. Accordingly, we may anticipate their electrostatic interactions with DNA to be similar while differing in both thermal phase behaviour and physicochemical properties of their complexes with DNA. In keeping with the above all three lipids formed complexes with DNA as evidenced by light scattering, fluorescence spectroscopy and Langmuir film balance. Differential scanning calorimetry revealed very different phase behaviours for the binary mixtures of the three CLs with dimyristoylphosphatidylcholine and also provided evidence for DNA-induced lipid phase separation. These data were confirmed by compression isotherms and fluorescence microscopy of monolayers residing on an aqueous buffer, recorded both in the presence and absence of DNA. Importantly, binding to cationic liposomes appears to prevent thermal denaturation of DNA upon heating of the complexes. Likewise, renaturation of heat-treated DNA complexed with the cationic liposomes appears to be abolished as well.

Abbreviations: Adr, adriamycin; Adr–DNA, adriamycin–DNA complex; BBDAB, bis[2-(11-butyloxyundecanoate)ethyl]dimethylammonium bromide; BPDAB, bis[2-(11-phenoxyundecanoate)ethyl]dimethylammonium bromide; bisPDPC, 1,2-bis[(pyren-1-yl)decanoyl]-*sn*-glycero-3-phosphocholine; CL, cationic lipid; DCC, dicyclohexylcarbodiimide; DSC, differential scanning calorimetry; DMAP, dimethylaminopyridine; DMPC, 1,2-dimyristoyl-*sn*-glycero-3-phosphocholine; DOPE, 1,2-dioleoyl-*sn*-glycero-3-phosphoethanolamine; DPPC, 1,2-dipalmitoyl-*sn*-glycero-3-phosphocholine; ds-DNA, double stranded DNA; EDTA, ethylenediaminetetraacetic acid; HADAB, *N*-hexadecyl-*N*-{10-[*O*-(4-acetoxy)phenylundecanoate]ethyl}dimethyl ammonium bromide; HEPES, *N*-(2-hydroxyethyl)piperazine-*N*′-2-ethanesulphonic acid; LUV, large unilamellar vesicle; MLV, multilamellar vesicle; NMR, nuclear magnetic resonance; NBD-PC, 1-palmitoyl-2-{12-[(7-nitro-2-1,3-benzoxadizol-4-yl)amino]dodecanoyl)-*sn*-glycero-3-phosphocholine; PC, phosphatidylcholine; TLC, thin layer chromatography; T_m, lipid main transition temperature; T_p, lipid pretransition temperature; π, surface pressure; ΔH, transition enthalpy

* Corresponding author. Fax: +358-9-191-8276; E-mail: paavo.kinnunen@helsinki.fi

[1] A preliminary account of the key findings of this study was communicated in the 25th FEBS 98 Silver Jubilee Meeting, July 5–10, 1998, held in Copenhagen, Denmark.

[2] Present address: Department of Chemistry, Emory University, Atlanta, GA 30322, USA.

0005-2736/00/$ – see front matter
PII: S0005-2736(00)00183-8

Keywords: Cationic lipid; DNA; Liposome; Phase behavior; Monolayer; Fluorescence microscopy

1. Introduction

Liposome-based transfection systems provide certain advantages over viral vectors in gene therapy, including non-immunogenicity, lack of biohazards and the possibility for introducing larger DNA fragments into target [1–7]. Accordingly, intense efforts continue to be undertaken to elucidate optimal structures of DNA/cationic liposome complexes and their mechanism(s) of delivery of DNA into cells (e.g. [8–19]). Formation of liposome–DNA complexes (lipoplexes) followed by an incubation with the target cells is needed for transfection. Although electrostatic association between cationic lipid (CL) headgroups and the negatively charged phosphates of DNA provides the primary driving force for complex formation, other interactions also seem to contribute [20–22]. The binding of CLs to DNA causes its condensation and the formation of compact, dense structures [23–30], revealed by electron [13,23,31,32] as well as atomic force microscopy [33]. Several models have been suggested for the structure of the CL/DNA complexes [14,32–37]. Moreover, the available data indicate that the lipid-to-DNA ratio as well as lipid composition can critically affect the transfection efficiency of these delivery vehicles (e.g. [38,39]). Also the form of liposomes in transfection efficiency is important and in addition to the DNA/CL ratio, sonication and heating, as well as unilamellarity of the liposome, enhanced the delivery of genetic material [38].

It has been shown that CL–DNA complexes form a multilamellar structure composed of alternating lipid bilayer and DNA monolayer with distinct interhelical DNA spacings [28]. It was further also demonstrated that altering the lipid-to-DNA mass ratio induced two regimes for the complex size and surface charge [40] which correspond to regimes of either excess DNA or lipid. Xu et al. studied the morphology of *N*-[1-(2,3-dioleoyloxy)propyl]-*N*,*N*,*N*-trimethyl ammonium salt liposomes with electron microscopy [41] and observed that neat lipid vesicles were spherical whereas the addition of DNA deformed the vesicles into high curvature structures, which were further influenced by the lipid composition. Interestingly, the isolated positively charged complexes showed high transfection efficiency compared to the starting mixtures. Another study demonstrated that DNA adsorbed to oppositely charged lipid bilayer can adhere neighbouring vesicle membranes [42]. At low DNA content, large multilamellar CL–DNA complexes were formed whereas at high DNA content the aggregation and flattening of unilamellar vesicles was evident. Both of the above CL–DNA complexes exhibited partially open bilayer segments with DNA accumulated on the edges [42]. Upon binding of DNA to the lipid membranes DNA can undergo a structural transition from B to C form [43]. CLs may also form hydrophobic complexes with DNA, allowing for the subsequent assembly of particles in which DNA is no longer condensed [26,27]. Conformational changes in DNA induced by CLs have been reported to depend on lipid structure as well as temperature [44] and the condensed DNA bound to cationic liposomes is protected from the action of DNase I [18,38].

The mechanism(s) of entry of the DNA contained in lipoplexes into cells remain(s) to be established. There is evidence for endocytosis being involved [1,12,45,46]. Inverted non-lamellar phase forming lipids such as 1,2-dioleoyl-*sn*-glycero-3-phosphoethanolamine (DOPE) [9,46,47] and diacylglycerol [19] promote the uptake of DNA by cells. Both of these H_{II} phase forming lipids are intimately connected to the molecular mechanism of membrane fusion [48] and the involvement of this process in cellular transfection by lipoplexes has been proposed [16,49]. Recently, release of DNA from cationic lipoplexes by anionic lipids in cell membranes has been demonstrated [14]. These data are supported by the in vitro observation of release of DNA from complexes with cationic liposomes by acidic phospholipids [14,50].

The nature and consequences of interaction of CL with DNA may not only be relevant to the understanding of the transfection process. While the biological significance of this finding remains open, the natural cationic bioactive lipid, sphingosine, has been shown to bind to DNA, forming 'beads on a string'

structures as well as larger aggregates [21,22,51]. This interaction is driven electrostatically and can be reversed by phosphatidic acid, another bioactive lipid [50]. Lipid phase separation was demonstrated to take place upon the binding of DNA as well as RNA to sphingosine containing liposomes [21,22,51]. DNA has a profound influence on the thermal phase behaviour of sphingosine containing liposomes as well as on the lateral packing of monolayers [52].

In keeping with the above it has become clear that elucidation of the physical properties of liposomal vectors is essential in order to optimise this process. In this paper we characterise the thermal phase behaviour of 1,2-dimyristoyl-*sn*-glycero-3-phosphocholine (DMPC) alloyed with three CLs, bis[2-(11-phenoxyundecanoate)ethyl]dimethylammonium bromide (BPDAB), *N*-hexadecyl-*N*-{10-[*O*-(4-acetoxy)phenyl-undecanoate]ethyl} dimethylammonium bromide (HADAB) and bis[2-(11-butyloxyundecanoate)ethyl]-dimethylammonium bromide (BBDAB). Fluorescence spectroscopy, lipid monolayers and fluorescence microscopy were used to observe the binding of DNA to these CL and differential scanning calorimetry (DSC) to study the effects of DNA on the phase behaviour of the CL/DMPC combinations.

2. Experimental procedures

2.1. Materials

Calf thymus DNA, DMPC, 1,2-dipalmitoyl-*sn*-glycero-3-phosphocholine (DPPC), *N*-(2-hydroxyethyl)piperazine-*N*′-2-ethanesulphonic acid (HEPES) and ethylenediaminetetraacetic acid (EDTA) were from Sigma. 1,2-Bis[(pyren-1-yl)decanoyl]-*sn*-glycero-3-phosphocholine (bisPDPC) was from K&V Bioware (Espoo, Finland). 1-Palmitoyl-2-{12-[(7-nitro-2-1,3-benzoxadizol-4-yl)amino]dodecanoyl}phosphocholine (NBD-PC) was from Avanti Polar Lipids (Alabaster, AL, USA). *N*-Methyldiethanolamine, *N*,*N*-dimethylethanolamine, 1-bromohexadecane, 11-bromoundecanoic acid, dicyclohexylcarbodiimide (DCC) and dimethylaminopyridine (DMAP) were from Fluka (Buchs, Switzerland). The purity of the lipids was checked by thin layer chromatography (TLC) on silicic acid coated plates (Merck, Darmstadt, Germany) using chloroform/methanol/water (65:25:4, by volume) as a solvent system for the above phospholipids and chloroform/methanol (9:1, by volume) for the CLs. Examination of the TLC plates after iodine staining or, when appropriate, by fluorescence illumination revealed no impurities. Concentrations of phospholipids were determined by the phosphorus assay [53] and those of the CLs gravimetrically using a high precision electrobalance (Cahn, Cerritos, CA, USA). DNA concentrations (in mM basepairs) were determined by absorbance at 260 nm ($\varepsilon = 6600$ l/mol cm) and by the phosphorus assay. Freshly deionised filtered water (Milli RO/Milli Q, Millipore, Jaffrey, NH, USA) was used in all experiments. The cationic liposome/DNA complexes were made by mixing the hydrated lipid and DNA at the indicated molar ratios.

2.2. Synthesis of the CLs

BPDAB and BBDAB were synthesised and purified as described in detail elsewhere [54]. In brief, *N*-methyldiethanolamine was coupled with the appropriate acid chloride to yield the corresponding diacylated products, *N*,*N*-(diacyloxyethyl)methylamines. Quaternisation of these amines by treatment with dimethyl sulphate followed by potassium bromide furnished the quaternary ammonium bromide surfactant lipids, BPDAB and BBDAB. The amide lipid, HADAB, was synthesised as follows. Treatment of *N*,*N*-dimethylethanol amine with 1-hexadecyl bromide in dry acetone yielded dimethyl-[*N*-hexadecyl-*N*-(2-hydroxyethyl)]ammonium bromide, m.p. 176°C with quantitative (100%) yield after recrystallisation from acetone/hexane (10:1, by volume). 11-(4-Acetoxy)phenyl-undecanoic acid was prepared by reacting 11-bromoundecanoic acid with *p*-hydroxyacetanilide in the presence of NaOH. Dimethyl-[*N*-hexadecyl-*N*-(2-hydroxyethyl)]ammonium bromide was subsequently acylated with 11-(4-acetoxy) phenylundecanoic acid in the presence of DCC and DMAP in freshly distilled $CHCl_3$ (dried over P_2O_5) to give HADAB. The product was purified on a silica gel column eluted with $CHCl_3$–MeOH (94:6, by volume). Yield of the colourless solid (m.p. 105–108°C) was 85%. Chromatographically purified product revealed by infrared, ^{1}H-NMR (nuclear magnetic

resonance) and elemental analysis consistent with HADAB.

2.3. Preparation of liposomes

Multilamellar liposomes (MLVs) were prepared by mixing appropriate amounts of the lipid stock solutions in dry chloroform to formulate the desired compositions. Thereafter the solvent was removed by evaporation under a stream of nitrogen. For removal of residual amounts of solvent the samples were further maintained under high vacuum for at least 2 h. The resulting dry lipid films were then hydrated with 5 mM HEPES, 0.1 mM EDTA, pH 7.4 and thereafter incubated for 30 min above the main transition temperature of the lipid components (approximately 70°C). To obtain large unilamellar vesicles (LUVs, diameter approximately 100 nm) the hydrated lipid dispersions were vortexed vigorously and then extruded with a Liposo-Fast small volume homogeniser (Avestin, Ottawa, Canada) by subjecting to 19 passes through a stack of two polycarbonate filters (100 nm pore size, Nucleopore, Pleasanton, CA, USA) installed in tandem.

2.4. Differential scanning calorimetry

These measurements were performed with a Privalov high-sensitivity adiabatic differential scanning calorimeter (DASM-4, Biopribor, Pushchino, Russia) at a heating rate of 0.5°C/min. The instrument was interfaced to a 486 PC via DT01-EZ data acquisition board (Data Translation, Marlboro, MA, USA) and data were analysed using the routines of the Origin software (Microcal, Northampton, MA, USA). MLVs were vortexed and kept on an ice waterbath for at least 12 h before loading into the calorimeter cuvette. When indicated double stranded DNA (ds-DNA) was added to MLVs and kept on an ice bath prior to DSC measurements.

2.5. Transmission electron microscopy

Suspensions of the CLs (approximately 2 mM in 5 mM HEPES, 0.1 mM EDTA, pH 7.4) were applied to a carbon grid, stained with 1% uranyl acetate and viewed with a Jeol JEM-100S transmission electron microscope (JEOL, Tokyo, Japan) at a magnification of 10 000×.

2.6. Fluorescence measurements

Fluorescence measurements were carried out with a Perkin-Elmer LS 50B spectrometer interfaced to a Compaq 486 Prolinea 4/25s computer. BisPDPC ($X=0.01$) was utilised to measure the binding of adriamycin (Adr)-labelled DNA to liposomes [21,22,51]. In brief, solutions of DNA and Adr were mixed in 5 mM HEPES, 0.1 M EDTA, pH 7.4 buffer to obtain a DNA–Adr complex with a nucleotide/Adr ratio of 8:1. Subsequently, the liposome solution was divided into proper aliquots and diluted with buffer to yield a final lipid concentration of 25 μM.

Excitation wavelength for the pyrene-labelled lipids was 344 nm while 5 nm bandwidth was used for both excitation and emission. Two ml of CL/DMPC liposome solution was applied to a magnetically stirred four-window quartz cuvette placed in a thermostated compartment. The temperature was controlled by a circulating water bath. Emissions at ~380 and 480 nm were taken for the pyrene monomer (I_m) and excimer intensities (I_e), respectively. Changes in the emission intensity due to the binding of Adr–DNA to liposomes were measured after allowing the samples to stabilise for 5 min after each addition. All binding experiments were carried out at 30°C and the fluorescence intensity values were corrected for dilution.

2.7. Light scattering measurements

Static light scattering due to DNA–cationic complex formation was measured with the spectrofluorometer with the excitation and emission monochromators set at 500 nm. 2 ml of 100 μM 1:1 CL/DMPC LUVs was placed in a magnetically stirred four-window quartz cuvette thermostated at 30°C. Scattering intensities were measured 5 min after the addition of ds-DNA to the indicated concentrations and were found to remain constant after this period.

2.8. Monolayer experiments

Compression isotherms were recorded using a miniature Langmuir trough (μTrough S, Kibron, Helsin-

ki, Finland) monitoring surface pressure by the Wilhelmy technique. The compression rate was controlled and the values of surface area and surface pressure were collected by a computer operated with FilmWare, dedicated software provided by the instrument manufacturer. Lipid mixtures of the desired compositions were prepared by mixing the appropriate amounts in chloroform and were spread on the air–buffer (5 mM HEPES, 0.1 mM EDTA, pH 7.4) interface with a microsyringe. Monolayers were allowed to equilibrate for 10 min for evaporation of the solvent before starting the compression. All isotherms were measured at ambient temperature (24 ± 1°C) and at a constant compression rate of 4 Å^2/acyl chain/min. When indicated 2.5 μM DNA (in basepairs) was included into the subphase.

2.9. Fluorescence microscopy of monolayers

Lateral organisation of CL/DPPC monolayers was observed by fluorescence microscopy and using a computer controlled Langmuir-balance, as described above. The total surface area of the trough was 120 cm^2 and the volume of the subphase was 22 ml. The trough was mounted on the stage of an inverted microscope (Zeiss IM-35) and the quartz-glass window in the bottom of the trough was positioned over an extra long working distance 20× objective. A 450–490 nm bandpass filter was used for excitation and a 520 nm longpass filter for emission. Images were viewed with a Peltier-cooled 12-bit CCD camera (C4742-95, Hamamatsu, Japan) interfaced to a computer (Pentium 166 MHz) and running image processing software provided by the camera manufacturer (HiPic, 4.2.0). One mole percent of NBD-PC was used as a fluorescent probe. Stock solutions of the probe and the lipids, DPPC/BPDAB/NBD-PC, at the indicated molar ratios (89:10:1, 79:20:1 and 69:30:1) and DPPC/HADAB/NBD-PC (89:10:1, 79:20:1 and 69:30:1) were prepared in chloroform and stored at −20°C. These mixtures were applied on the air–buffer (5 mM HEPES, 0.1 mM EDTA, pH 7.4) interface using a Hamilton microsyringe to initial areas of 100 ± 10 Å^2/acyl chain. After an equilibration period of 10 min the monolayers were compressed symmetrically using two barriers at a rate of 2.5 Å^2/acyl chain/min. After reaching the indicated values for surface pressure (π) the compression was stopped and the monolayer was allowed to settle for 2 min prior to recording the image. When indicated 2.5 μM ds-DNA (in basepairs) was included into the subphase. All measurements were carried out at an ambient temperature of 24 ± 1°C.

3. Results

The chemical structures of the three CLs, BPDAB, BBDAB and HADAB, are compiled in Fig. 1. All three compounds could be readily dispersed into aqueous buffers, forming opalescent suspensions. Upon DSC dispersions of BPDAB, BBDAB and HADAB exhibited endotherms at 44.3, 11.6 and 54°C, respectively, with the corresponding total enthalpies of 7.2, 6.2 and 2.0 kcal/mol. It was previously shown that BPDAB and BBDAB form vesicles with diameters of 1530 ± 100 and 800–1000 Å, respectively [54]. Our transmission electron microscopy images revealed BPDAB to form rodlike long structures, whereas both BBDAB and HADAB form large multilamellar vesicles (with approximate aver-

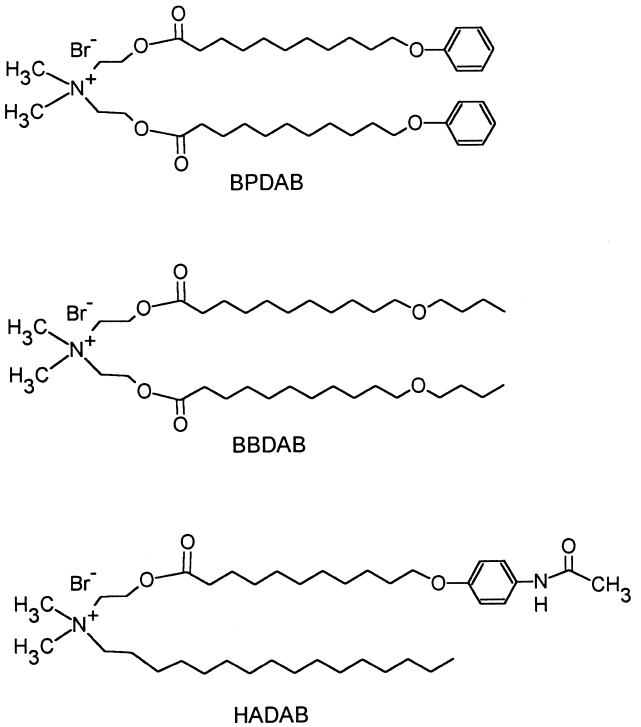

Fig. 1. Structures of CLs BPDAB, BBDAB and HADAB used in this study.

age diameters of 3000 and 9000 Å, respectively, data not shown).

3.1. Formation of DNA–CL complexes

As expected, binary liposomes containing the above CLs and DMPC bound DNA. This could be readily observed by light scattering measurements for the three cationic amphiphiles alloyed with DMPC at 1:1 molar ratio, shown as a function of [DNA], so as to yield varying nucleotide/CL stoichiometries (Fig. 2). Binary liposomes of BPDAB, BBDAB and HADAB with DMPC scattered only weakly and constant signals were measured even after prolonged incubations. Addition of ds-DNA to these LUVs produced rapid aggregation at DNA/CL molar ratios of 0.1 and 0.2. The maximum extent of scattering did depend on the CL used and both BPDAB/DMPC and BBDAB/DMPC LUVs showed higher scattering intensities than liposomes containing HADAB. Enhanced scattering measured upon increasing the

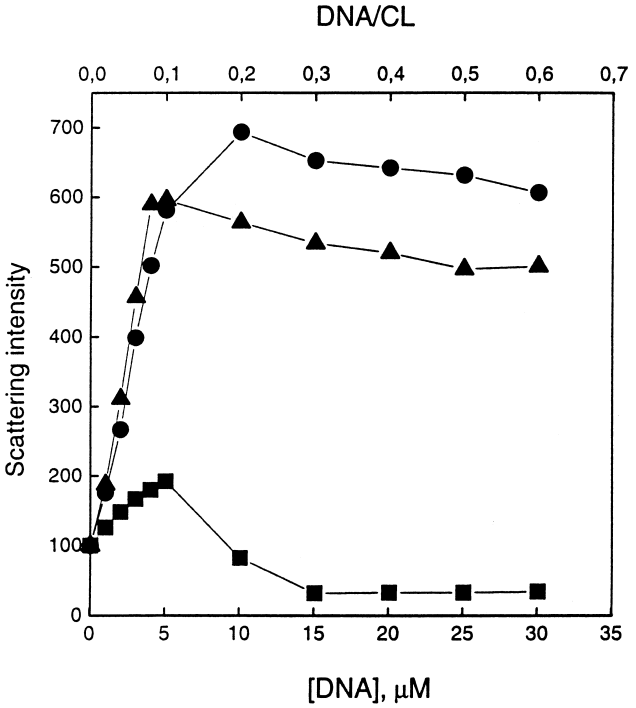

Fig. 2. Light scattering for DNA/lipid complexes as a function of the DNA/CL mole ratio. CL/DMPC (1:1 molar ratio) LUVs were BPDAB/DMPC (●), BBDAB/DMPC (▲) and HADAB/DMPC (■). Scattering intensity data were measured 5 min after the addition of ds-DNA at 30°C. Total lipid concentration was 0.1 mM in 5 mM HEPES, 0.1 mM EDTA, pH 7.4.

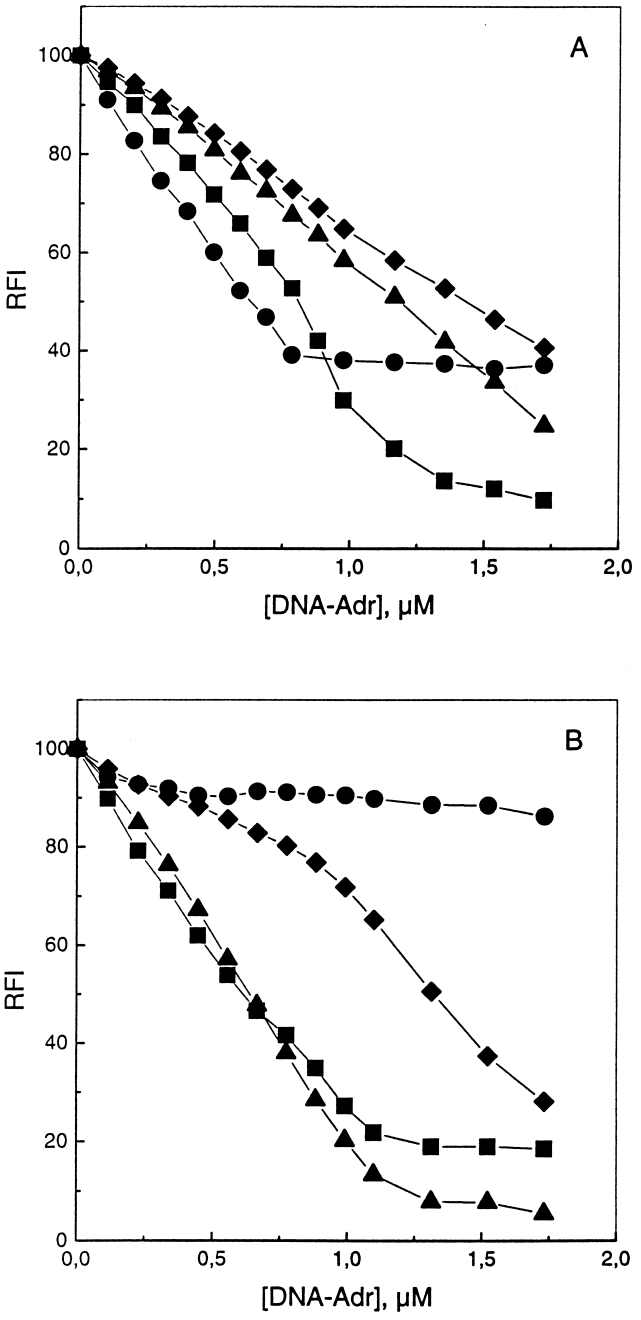

Fig. 3. Binding of ds-DNA to CL/DMPC/bisPDPC LUVs monitored by a decrease in relative fluorescence intensity (RFI) of the pyrene-labelled lipid due to quenching by Adr-labelled DNA. The mole fraction of the CL BPDAB (A) or HADAB (B) in liposomes was 0.05 (●), 0.10 (■), 0.20 (▲) or 0.30 (♦). Temperature was maintained at 30°C. Buffer was 5 mM HEPES, 0.1 mM EDTA, pH 7.4 and the total concentration of lipid was 25 μM.

DNA/CL ratio from 0.0 to 0.1 indicates an increasing size of the DNA/liposome complexes. The DNA–lipid complexes formed by BPDAB and BBDAB were stable and did not precipitate. For HADAB, however, a pronounced decrease in light scattering was evident at DNA/HADAB molar ratios exceeding 0.1, indicating precipitation of the DNA–lipid complexes.

Binding of DNA to the CL containing liposomes was confirmed using fluorescence measurements. This is illustrated in Fig. 3 for LUVs containing varying mole fractions of either BPDAB (panel A) or HADAB (panel B). In brief, with an increase in X_{CL} resonance energy transfer from the pyrene-labelled lipid (donor) to the Adr-labelled DNA (acceptor) [21,22,51] resulted in a progressively enhanced fluorescence quenching for the donor. Negligible quenching was evident for liposomes lacking the CLs (data not shown). The degree of quenching of pyrene excimer fluorescence by Adr–DNA upon its binding to BPDAB/DMPC LUVs was dependent on X_{BPDAB}. More specifically, increasing X_{BPDAB} from 0.05 to 0.10 increased the maximum extent of resonance energy transfer. However, upon increasing X_{BPDAB}, progressively higher concentrations of Adr–DNA were required for half-maximal quenching. The binding of DNA to BPDAB/DMPC liposomes saturated at DNA/CL molar ratios between 0.5 and 0.6, irrespective of the content of BPDAB in the liposomes. This result suggests that DNA may initially interact only with the outer monolayer of the liposome. A somewhat different behaviour was evident for HADAB. Accordingly, $X_{HADAB} = 0.05$ was insufficient for significant binding of DNA to liposomes. Increasing X_{HADAB} to 0.10 saturation was evident at DNA/HADAB molar ratios in the range of 0.2 and 0.4. These measurements were performed at 30°C. This choice of temperature was somewhat arbitrary as the effect of lipid phase state was not assessed.

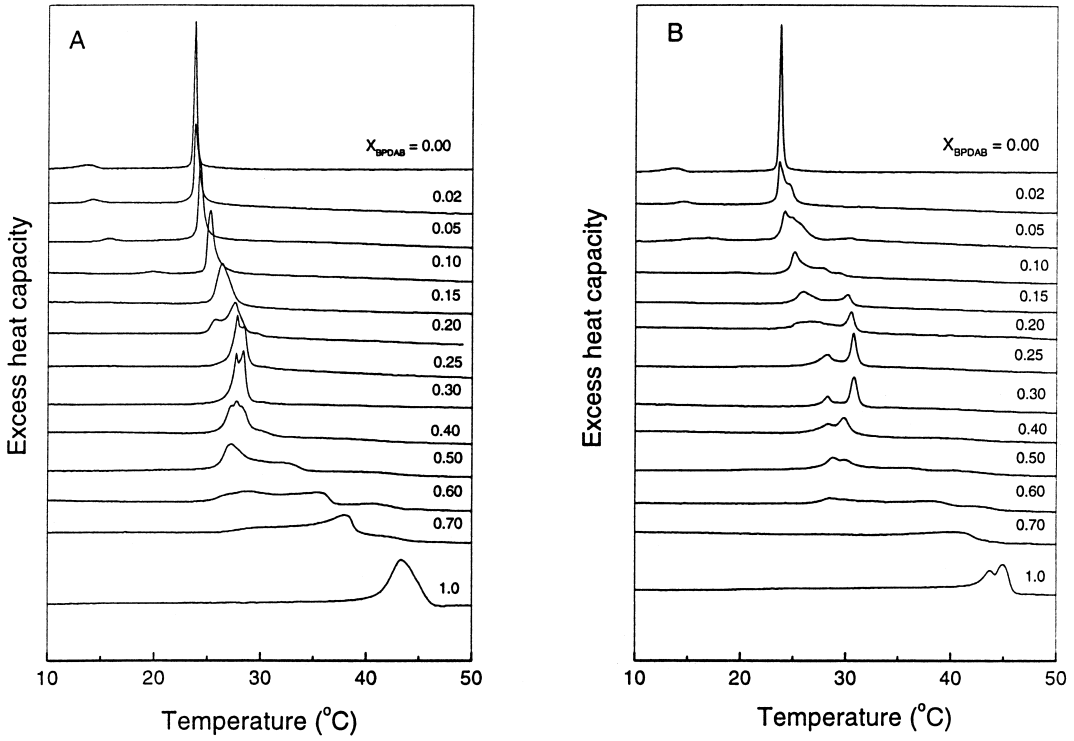

Fig. 4. (A) DSC traces for BPDAB/DMPC MLVs with the indicated mole fractions of BPDAB. Total lipid concentration was 1 mM in 5 mM HEPES, 0.1 mM EDTA, pH 7.4. (B) Thermograms measured for these BPDAB/DMPC MLVs after incubation with 0.2 mM ds-DNA.

3.2. Thermal phase behaviour of BPDAB/DMPC liposomes and effects of DNA

Representative DSC heating thermograms for binary BPDAB/DMPC liposomes with increasing X_{BPDAB} are shown in Fig. 4A. Neat DMPC exhibits two transitions, pretransition at $T_p \approx 15°C$ and main transition at $T_m \approx 23°C$. Increasing the mole fraction of BPDAB from 0 to 0.10 increases T_p from 15 to 20°C, with a concomitant decrease in pretransition enthalpy. At $X_{BPDAB} > 0.15$, pretransition could no longer be resolved. Simultaneously, when X_{BPDAB} was increased from 0 to 0.20, the main transition endotherm revealed two broad components with a maximum at 26.5°C and a combined enthalpy ΔH_m of 6.5 kcal/mol. At $X_{BPDAB} = 0.25$ the binary mixture exhibits a high temperature shoulder at 28.4°C. Upon further increase of X_{BPDAB} to 0.30 the higher temperature endotherm becomes more distinct. At a BPDAB/DMPC molar ratio of 1:1, three broad and overlapping endotherms are present. The peak at 27.3°C is likely to be due to domains enriched in DMPC. Likewise, the transition at 40.1°C should be caused by the melting of domains enriched in BPDAB. Between these a broad endotherm centred at 32.1°C is likely to result from the lipidic BPDAB/DMPC mixed phase. Non-ideal mixing is seen at higher contents of BPDAB, with broad, overlapping endotherms being evident.

Subsequently, it was of interest to study the effects of DNA on the BPDAB/DMPC liposomes. In the first series of experiments the concentration of DNA was kept constant at 0.2 mM while X_{BPDAB} was varied (Fig. 4B). DNA caused no changes in the melting temperature of neat DMPC liposomes, in keeping with lack of interaction of DNA with this zwitterionic lipid. As expected from the binding of DNA to the CL containing liposomes as well as on the basis of previous DSC-studies on similar systems, pronounced effects on the thermal phase behaviour of BPDAB/DMPC alloys were evident (Fig. 4B). At $X_{BPDAB} = 0.02$ to 0.10 the presence of DNA increases T_p slightly, by $\sim 0.1°C$, whereas at $X_{BPDAB} = 0.15$ the pretransition can no longer be observed similarly to BPDAB/DMPC mixtures. For the main transition at $X_{BPDAB} = 0.02$ a higher temperature shoulder at 24.6°C as well as broadening of the peak was induced by DNA. Upon increasing X_{BPDAB} to 0.05 and 0.10 the formation of a DNA–CL complex was evident as further broadening of the original main transition peak with a minor increase in T_m ($\sim 24.2°C$). At $X_{BPDAB} = 0.15$ a new endotherm at 29.9°C was induced by DNA, indicating the formation of a separate domain enriched in the CL and with bound DNA. Concomitantly, the endotherm at 26.2°C for membrane enriched in DMPC became sharper. The enthalpies of the CL–DNA complex

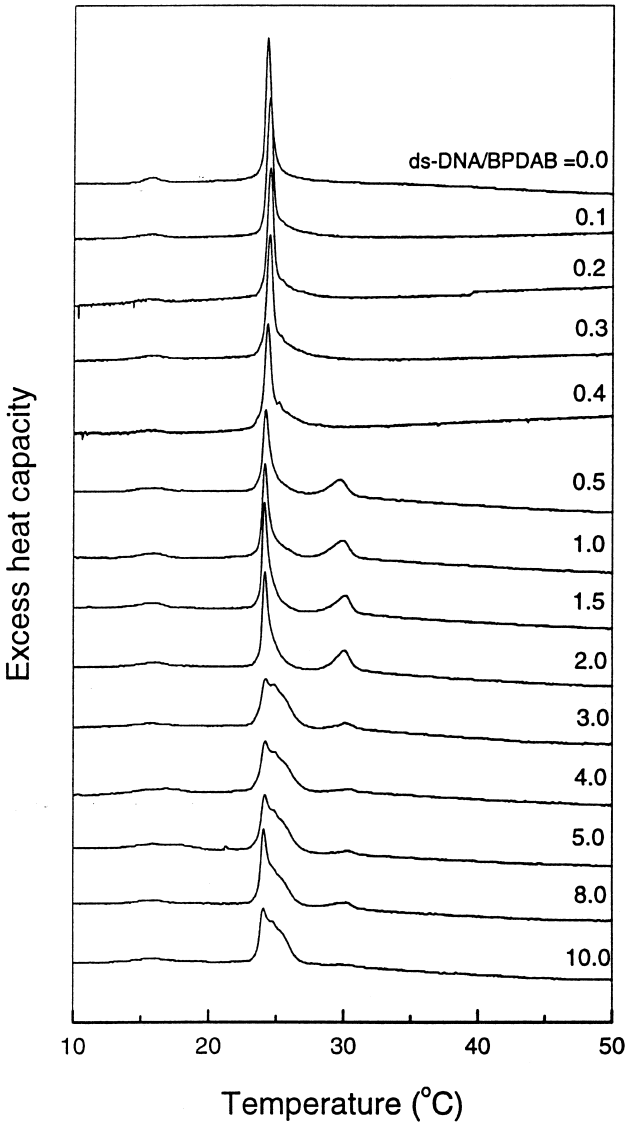

Fig. 5. Effect of increasing [ds-DNA] on the phase behaviour of BPDAB/DMPC (5:95, molar ratio) liposomes. Total lipid concentration was 1 mM in 5 mM HEPES, 0.1 mM EDTA, pH 7.4. The nucleotide/BPDAB molar ratio is given above each corresponding thermogram.

and the DMPC enriched phase were 1.2 and 2.5 kcal/mol, respectively. Increasing X_{BPDAB} to 0.20 increased the magnitude of the endotherm for the CL–DNA complex at 30.4°C. When X_{BPDAB} was increased further to 0.25 and 0.30 the phase separation due to DNA became more pronounced and two endotherms at 30.7 and 30.8°C were present. The addition of 0.2 mM DNA to neat BPDAB liposomes caused two peaks, again demonstrating segregation of the CL–DNA complex. The enthalpies of the two endotherms at 43.6 and 45°C were 4.2 and 2.2 kcal/mol, respectively. Cationic liposomes appear to prevent thermal denaturation of ds-DNA. When ds-DNA complexed with cationic liposomes was first heated above the melting temperature of ds-DNA (approximately 85°C) and after cooling subjected to a second DSC measurement, similar endotherms were evident as during the first scan for BPDAB/DMPC liposomes at $X_{BPDAB} = 0.10$ and at a nucleotide/CL molar ratio of 0.6 (data not shown).

The influence of increasing DNA concentrations on BPDAB/DMPC liposomes at $X_{BPDAB} = 0.05$ is shown in Fig. 5. These liposomes show pretransition at 16°C and main transition at 24.3°C, the latter with an enthalpy of 4.9 kcal/mol. Regardless of [DNA], pretransition and its enthalpy remained unaffected. Low concentrations of DNA (from 0.1 to 0.4 nucleotide/CL molar ratio) did not alter the main transition. Yet, a further increase in [DNA] gradually suppressed the main transition peak at 24.2°C. At a nucleotide/CL molar ratio of 0.5 the enthalpy of the main transition decreased to 3.41 kcal/mol and a new, well resolved endotherm at 29.2°C emerged, with an enthalpy of 1.61 kcal/mol. The combined enthalpy of the main transition and the DNA-induced endotherm (5.02 kcal/mol) was thus slightly higher compared to the main endotherm (4.94 kcal/mol) for the BPDAB/DMPC liposomes. Increasing [DNA] up to a nucleotide/CL molar ratio of 2 did not cause major changes either in the main transition or the higher temperature endotherm (Fig. 5). However, at a nucleotide/BPDAB molar ratio of 3 the main transition broadened and its enthalpy increased. Simultaneously, suppression of the endotherm at 30.6°C was evident. Further increasing [DNA] to yield a nucleotide/BPDAB molar ratio of 8 led to the broadening of the main transition and to the disappearance of the endotherm at 30°C.

To this end, although the structurally closely related CL BBDAB as such has a significantly lower

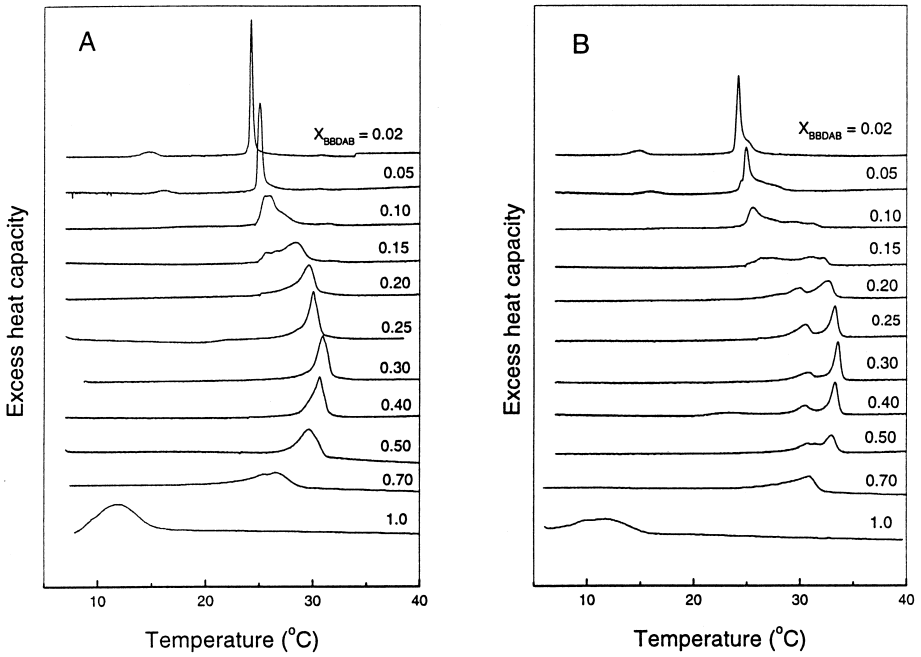

Fig. 6. Representative DSC heating scans for BBDAB/DMPC liposomes (1 mM, total lipid) with varying X_{BBDAB} in the absence (A) and presence (B) of 0.2 mM ds-DNA.

melting temperature (11.6°C) than BPDAB (44.3°C), a similar thermal behaviour to that of BPDAB is observed, when it is alloyed with DMPC, both in the absence and presence of DNA (Fig. 6). These data for BBDAB are not discussed in more detail.

3.3. Thermal phase behaviour of HADAB/DMPC liposomes and effects of DNA

Representative DSC heating thermograms for HADAB/DMPC MLVs at varying contents of this CL are compiled in Fig. 7A. At $X_{HADAB} = 0.02$, 0.05 and 0.10 the main transition DMPC is shifted to higher temperatures, 23.9, 25 and 26.1°C, respectively, with a concomitant decrease in ΔH from 4.8 to 4.2 and 4.0 kcal/mol, respectively. Unlike for BPDAB, the pretransition of DMPC is abolished already at $X_{HADAB} = 0.02$. At $X_{HADAB} = 0.15$ and 0.20 a non-ideal mixing of the two lipids was evidenced by the presence of two overlapping asymmetric endotherms. The influence of 0.2 mM ds-DNA on the thermal phase behaviour of HADAB/DMPC liposomes with an increasing content of CL is illustrated in Fig. 7B. Similarly to the other two CLs, DNA caused changes in the melting profiles of the liposomes indicative of phase separation. At $X_{HADAB} = 0.05$ two transitions at 24.4 and 26.4°C appeared. As X_{HADAB} was increased to 0.10, DNA caused both the main transition as well as the higher temperature endotherm to shift to higher temperatures. Increasing X_{HADAB} further to 0.15 and 0.30 resulted in a progressive reduction of the enthalpy of the main transition and a broadening of the higher temperature endotherm. No transitions were detected when X_{HADAB} exceeded 0.50.

3.4. Interaction of DNA with CL containing monolayers

Monolayers of the three CLs, BPDAB, HADAB and BBDAB, as neat films as well as mixed with DPPC at varying mole fractions were formed on the air/buffer interface and their compression isotherms were recorded both in the absence as well as in the presence of DNA in the subphase. DPPC was chosen for these studies since the T_m for this lipid is around 41°C and its main transition is readily observed in compression isotherms recorded at an ambient temperature of approximately 24°C. Accordingly, we anticipated any tendency for demixing

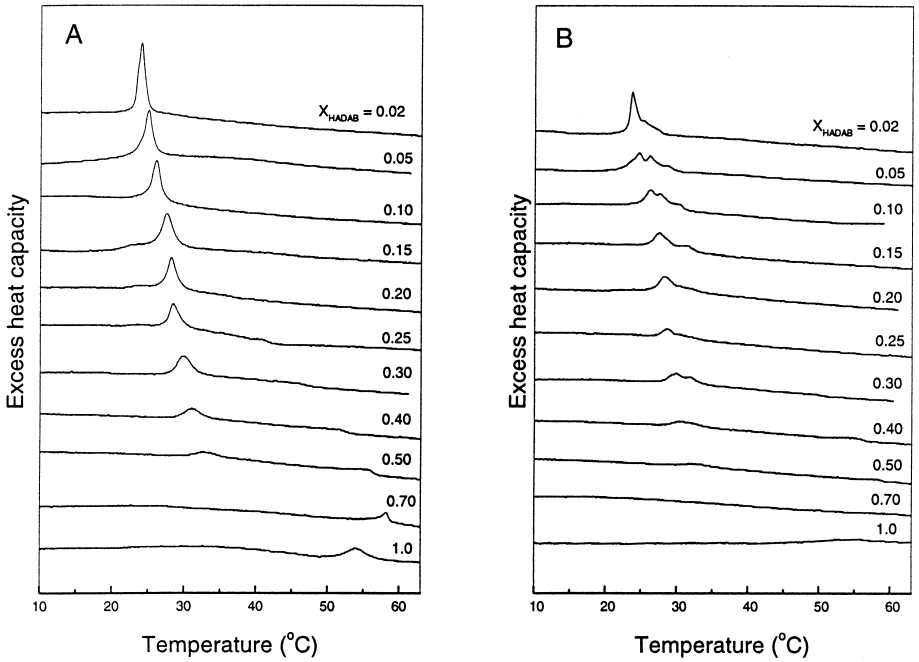

Fig. 7. DSC heating thermograms for HADAB/DMPC liposomes (1 mM total lipid) with the indicated contents of HADAB and in the absence (A) or presence (B) of 0.2 mM ds-DNA in 5 mM HEPES, 0.1 mM EDTA, pH 7.4 buffer.

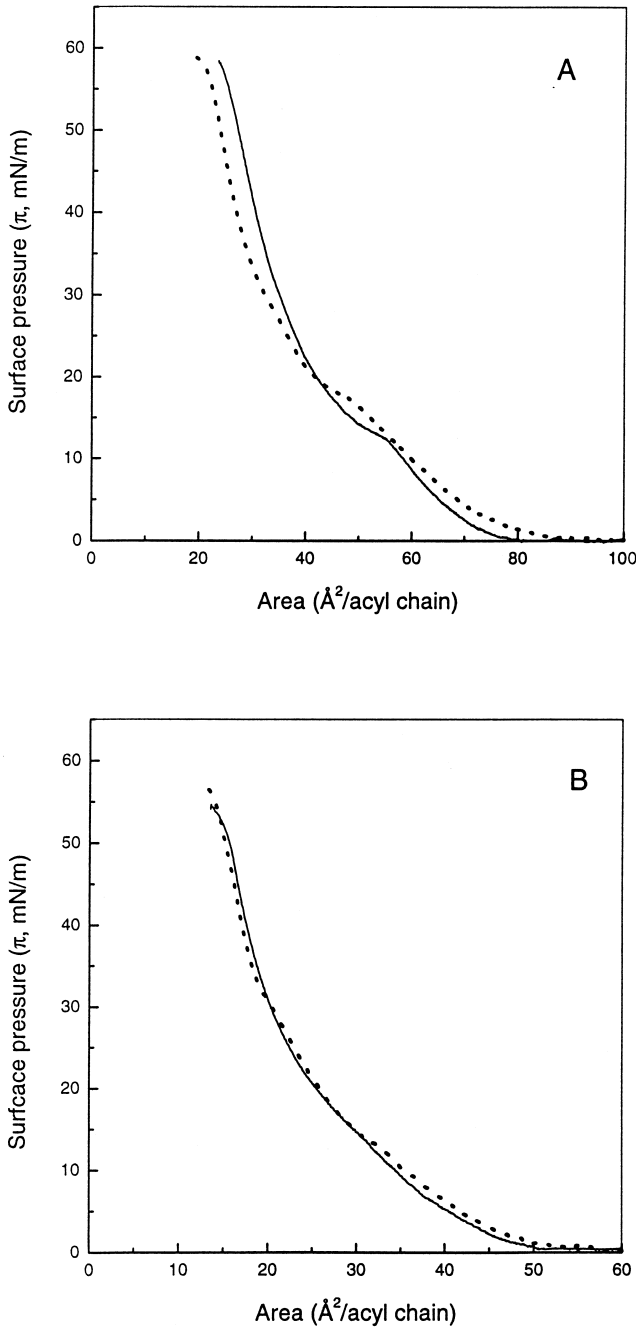

Fig. 8. Compression isotherms for DPPC monolayers at $X_{BPDAB} = 0.10$ (A) or X_{HADAB} (B) in the absence (solid line) and presence (dashed line) of 2.5 μM ds-DNA in the subphase. Compression rate was 4 Å²/acyl chain/min and the subphase was 5 mM HEPES, 0.1 mM EDTA, pH 7.4. Temperature was 24 ± 1°C.

to be detectable. Neat CLs formed stable films and produced smooth isotherms with collapse pressures of approximately 30 mN/m (data not shown). At $X_{BPDAB} = 0.10$ DPPC/BPDAB monolayers exhibited upon compression a discontinuity in the force/area curve at approximately 13 mN/m, thus indicating a transition between fluid and solid phases (Fig. 8A). A limiting area of 80 Å²/acyl chain was measured for this film. When 2.5 μM DNA was included into the subphase a discontinuity is evident at approximately 20 mN/m, in keeping with DNA induced phase separation in the monolayer and the appearance of a higher melting endotherm in DSC (Fig. 4). The nucleation of the condensed phase was shifted to a lower surface area of 25 Å² at 45 mN/m. These values can be compared to 35 Å² at 40 mN/m measured in the absence of DNA and are thus in accordance with DNA induced CL aggregation and reduced intermolecular repulsion due to charge neutralisation. Upon increasing X_{BPDAB} to 0.20 and 0.30, the phase separation caused by DNA, evident as discontinuity in the isotherm, shifted to still lower pressures, with a simultaneous decrease in collapse pressures (data not shown). A similar behaviour as described above for BPDAB was observed for BBDAB/DPPC monolayers (at X_{BBDAB} from 0.10 to 0.30), both in the presence and absence of DNA (data not shown).

Compared to BPDAB and BBDAB, isotherms for HADAB/DPPC films at $X_{HADAB} = 0.10$ revealed a lower value for the limiting area per molecule, 50 Å² (Fig. 8B). This could be attributed to a tighter packing between the molecules due to a decrease in intermolecular repulsion. Distinct from BPDAB and BBDAB, HADAB lacks the additional ether and ketone groups in one of the chains. The absence of such hydrophilic groups is in keeping with the diminished area/molecule measured for HADAB. When 2.5 μM DNA was present in the subphase a discontinuity in the isotherm was observed at 15 mN/m, in keeping with DNA-induced phase separation in the CL containing monolayer. Increasing the content of HADAB at $X = 0.20$ and 0.30 decreased the collapse pressure of HADAB/DPPC monolayers from 50 to 45 mN/m, respectively. However, at these molar ratios of HADAB the monolayers were unstable, i.e. they collapse at a significantly lower surface pressure compared to the other two CLs when DNA was included into the subphase.

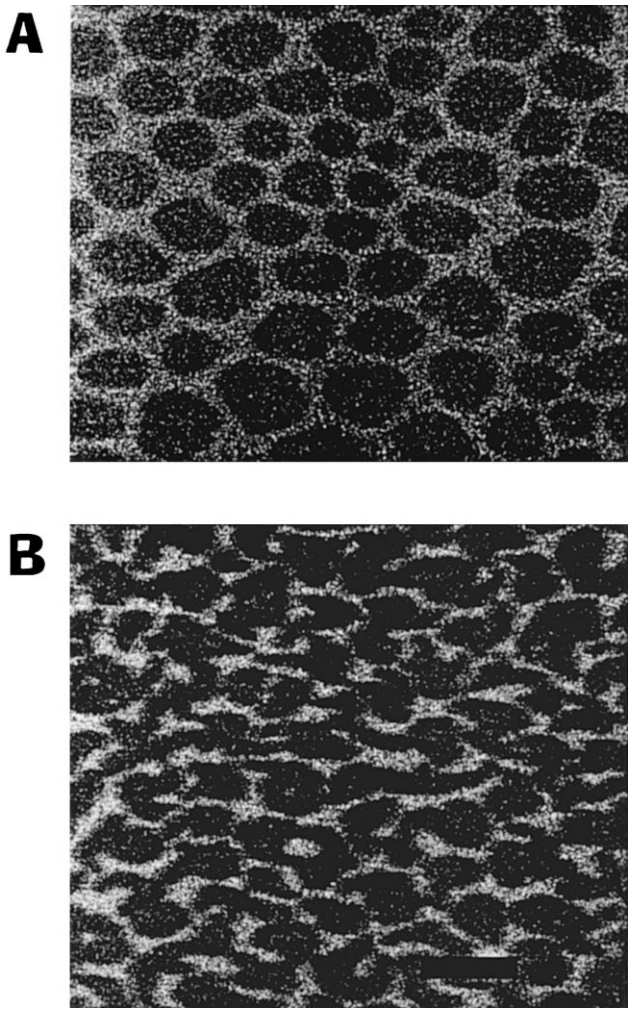

Fig. 9. Fluorescence microscopy images of a DPPC/BPDAB/NBD-PC (89:10:1, molar ratio) monolayer in the absence (A) and presence of 2.5 μM DNA (B) in the subphase at a surface pressure of 20 mN/m. Compression rate was 2.5 Å^2/acyl chain/min and the subphase was 5 mM HEPES, 0.1 mM EDTA, pH 7.4. Images were recorded at 24 ± 1°C. The scale bar in panel B corresponds to 20 μm.

Visual observation of coexisting solid and fluid phases in lipid monolayers by fluorescence microscopy requires the monolayers to contain a small amount of a proper fluorescent lipid marker, which preferentially partitions into the different phases [55,56]. To confirm the binding of DNA to monolayers we included a trace amount ($X = 0.01$) of the fluorescent phospholipid NBD-PC into mixtures of the different CLs with DPPC. Fluorescence microscopy images observed for DPPC/BPDAB/NBD-PC (89:10:1) monolayers with and without 2.5 μM DNA in the subphase and at surface pressure 20 mN/m are depicted in Fig. 9A,B, respectively. For monolayers on the buffer, small dark condensed domains were evident at surface pressures of 10–12 mN/m. These round domains became larger and uniformly distributed when π was increased to 25 mN/m. Above this pressure domains arranged into tightly packed arrays which were present up to the collapse at ~50 mN/m. When 2.5 μM DNA was present in the subphase, the dark domains appeared at 7–10 mN/m. Compared to the films on buffer domain morphologies observed in the presence of DNA were drastically different at higher packing densities (Fig. 9B). Domain morphologies were further dependent on the content of CL in the film. Accordingly, at $X_{BPDAB} = 0.20$ and 0.30 similar domain shapes were observed both in the presence and absence of DNA. We also investigated monolayers of DPPC/HADAB/NBD-PC at $X_{HADAB} = 0.10$ and 0.20 (data not shown). For these monolayers the formation of domain structures started in the surface pressure range of 20 to 25 mN/m. With buffer as the subphase and at $X_{HADAB} = 0.10$ small solid domains were observed at 25 mN/m. When 2.5 μM DNA was included into the subphase at surface pressures of 10–12 mN/m, domains with morphologies similar to those for BPDAB containing monolayers in the presence of DNA were evident. Yet, instability of the HADAB containing films in the presence of DNA prohibited meaningful experiments.

4. Discussion

The design of the formulations of cationic liposomes for cellular transfection has been empirical. Accordingly, there is little solid information showing what the relevant properties of the CLs are, except for the positively charged headgroup. Yet, a previous study [57] demonstrated that the acyl chain composition of CLs influences their transfection efficiencies. However, the phase behaviour of these lipids was not assessed in the above study. Starting at the level of chemical structures it was of considerable interest to investigate the impact of the hydrocarbon chains. The present study was undertaken in line with several earlier reports (e.g. [1–18]) to investigate the relationships between the physicochemical properties

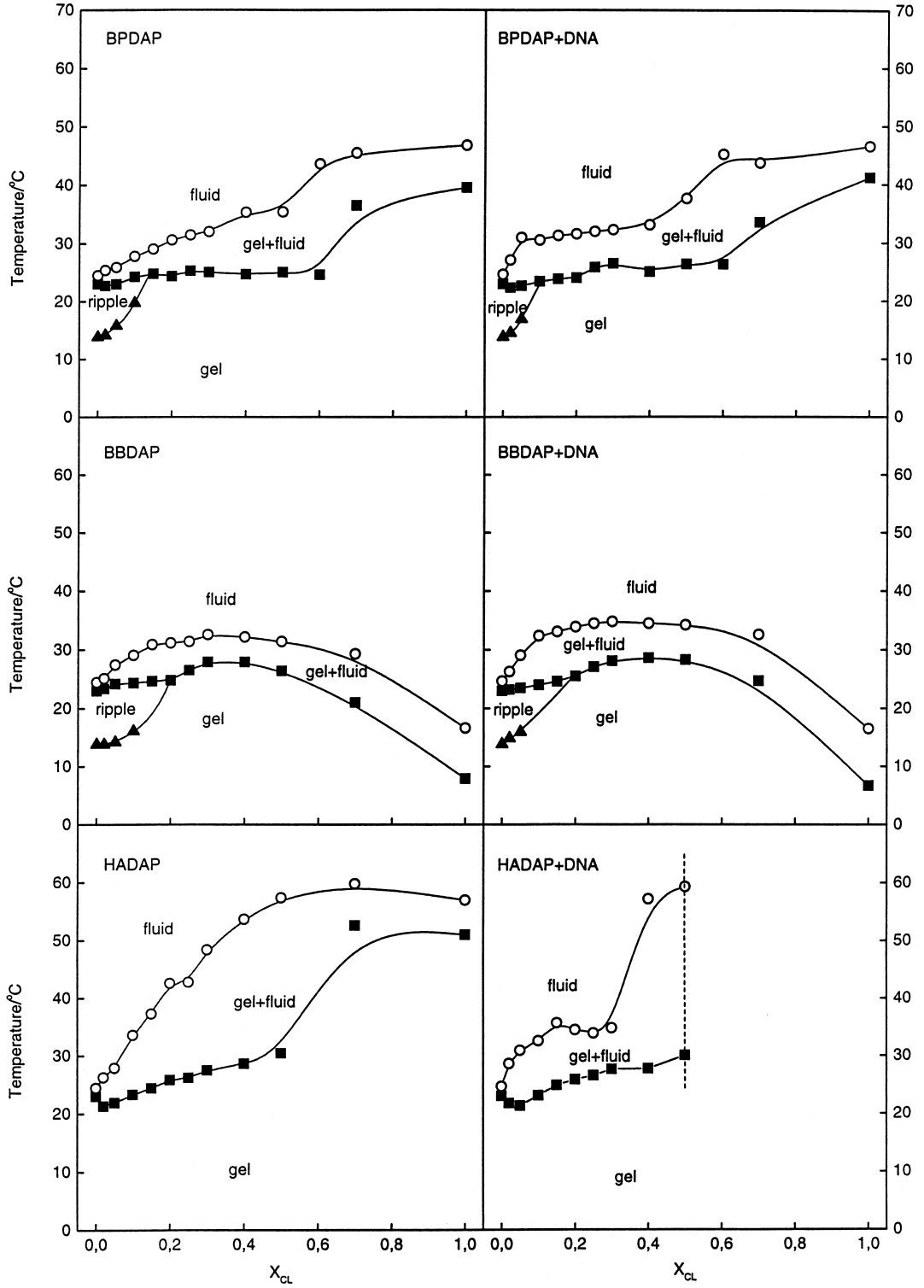

Fig. 10. Tentative phase diagrams derived from DSC for DMPC/BPDAB, DMPC/BBDAB and DMPC/HADAB MLVs in the absence (left panels) and presence (right panels) of DNA. The data were obtained from Figs. 4, 6 and 7.

of CLs and their complexes with DNA. Transfection efficiencies of these CLs will be addressed in a subsequent study (Paukku et al., to be published).

The lipids studied here (Fig. 1) bear identical cationic headgroups and either phenyl rings (BPDAB) or propyl moieties (BBDAB) in the ends of the two alkyl chains, or an alkyl chain and a phenyl ring with an amide group in the other chain (HADAB). Because of their identical headgroup we can assume these electrostatic interactions of the lipids with DNA to be identical. Instead, the different structures of their hydrophobic parts were anticipated to have a major impact on their thermal phase behaviour, as observed. We can assume the physicochemical properties of the different CLs to be reflected in their complexes with DNA. Accordingly, this should allow exploration of the dependence of the availability for cells of DNA in these complexes (Paukku et al., to be published) on their physicochemical characteristics (this study). We therefore first investigated the effects of DNA on the thermal phase behaviour of three novel CLs, BBDAB, BPDAB and HADAB [54], present as binary liposomes with DMPC.

Although the headgroup structure of lipids does affect the main transition, a major contribution is derived from the *trans-gauche* rotational isomerisation of the hydrocarbon chains [58]. Unlike the sharp transition characteristic to saturated phospholipids, the three CLs exhibit fairly broad enthalpy peaks, in keeping with diminished transition cooperativity. Compared to BBDAB introduction of the aromatic moiety increased T_m from 11.6 to 44.3°C for BPDAB and to 55°C for HADAB. The higher melting temperatures for the latter two lipids suggests stacking of the aromatic moieties to stabilise chain–chain interactions. Although the T_ms for BBDAB and BPDAB are different, the enthalpy of BBDAB, 6.2 kcal/mol, is rather close to that for the aromatic BPDAB. In comparison, while the T_ms for BPDAB and HADAB are rather close, their melting enthalpies, 7.2 and 2.0 kcal/mol, respectively, deviate significantly. The transitions of these lipids observed by DSC could basically represent either the gel-fluid or lamellar-hexagonal transitions. Except for HADAB the enthalpy values are rather large thus suggesting the former to be more likely. Moreover, an increase in light scattering upon heating was not observed (data not shown). The smaller ΔH of HADAB compared to the other two lipids is interesting. One possibility is that the hydrophilic *N*-acetoxy moiety could cause flipping of this chain of HADAB into the interfacial region [48], similar to that shown for the fluorescent lipid analog NBD-PC [59,60].

DSC data measured for DMPC/CL membranes at varying mole fractions of X_{CL} showed multiple endotherms, indicative of CL induced phase separation processes. Although well resolved endotherms were observed at DNA/CL molar ratios of 0.5–2 it should be emphasised that DSC data as such cannot be used to determine accurately the binding stoichiometry of the complex. The widening of the main transition peak upon increasing X_{CL} suggests a coexistence region, composed of fluid DMPC enriched domains and gel-like CL enriched domains. The similarity in the thermal phase behaviour (i.e. increase in T_m) of all three CLs combined with DMPC up to an X_{CL} of approximately 0.4 is somewhat unexpected, considering the overall differences in the phase behaviour of the neat CLs. This could originate from charge–charge repulsion between the CL headgroups dominating the melting behaviour of the alloy. Accordingly, only upon exceeding $X_{CL} \approx 0.4$ would the properties of the CL hydrocarbon chains be imparted on the phase behaviour of the alloy. Based on the DSC studies, preliminary phase diagrams were constructed (Fig. 10). It must be stressed, however, that DSC only detects changes in C_p and does not identify the actual phase states. The nature of the phases formed by these lipid mixtures thus remains uncertain at this stage. It is possible that some of these CLs could form or promote the formation of the inverted hexagonal phase H_{II}, particularly in the presence of DNA. Accordingly, the phase diagrams shown should be considered as tentative only. Nevertheless, judged from these data the phase behaviours of BPDAB and BBDAB remain rather similar in the absence and presence of DNA, in contrast to HADAB. For BPDAB and HADAB the addition of DNA promotes the formation of the fluid phase at $X_{CL} < 0.5$ whereas for BBDAB the opposite is observed.

All three CLs bind DNA avidly as demonstrated by the energy transfer as well as light scattering measurements. Results derived by the latter technique are consistent with the notion that BPDAB, BBDAB and HADAB bind to DNA up to a molar ratio of

about 0.1–0.2 DNA/CL (Fig. 2). Interestingly, for HADAB, increasing DNA concentrations so as to exceed the DNA/CL molar ratio of 0.2 resulted in a decrement in scattering intensity, indicating the precipitation of the complex. To this end, distinct from BBDAB and BPDAB, monolayers of HADAB were destabilised by DNA. Judged from light scattering at a DNA/CL molar ratio of 0.1, both BPDAB and BBDAB formed larger complexes than HADAB. Previous electron microscopy studies have revealed larger structures at lower DNA/CL ratios [61]. CLs forming rigid bilayers induce structural changes in DNA and it was further shown that the higher the T_m of the lipid, the greater the effect on DNA [44]. In contrast, fluidity of the CL membrane seems to promote close packing of condensed DNA [33]. Accordingly, different effects on DNA could also be anticipated for the CLs used in the present study, BBDAB, BPDAB and HADAB, with transition temperatures of 11.6, 44.3 and 54°C, respectively.

Segregation of DNA–CL complexes was evident in the thermal phase behaviour measured by DSC. This segregation was dependent on the DNA/CL molar ratio. For BPDAB/DMPC alloys, for instance, well resolved endotherms were evident at DNA/BPDAB molar ratios between 0.7 and 1.5 (Fig. 4B) thus supporting the notion that a DNA/CL ratio of 1.0 is optimal for binding of all the DNA by cationic liposomes, in keeping with previous studies [62,63]. Similar results were obtained for BBDAB. Also in this respect HADAB behaves differently from BPDAB and BBDAB and for this lipid phase separation is observed already at $X_{HADAB} = 0.05$, corresponding to a DNA/CL ratio of 0.25 (Fig. 7B).

Interestingly, compression isotherms for DPPC/HADAB monolayers with and without DNA are very similar. Intuitively one would expect that at low values of π an expansion in the area/molecule would be observed upon including DNA into the subphase. This is seen for both BPDAB and HADAB containing monolayers and could result from a partial intercalation of DNA into the monolayer. Alternatively, binding of DNA to the monolayer could more than compensate for the net positive damage of the film so as to cause the effective charge of the films with the attached DNA to be strongly negative. Accordingly, this would cause film expansion. Upon increasing π, DNA could be pushed out from the hydrocarbon region, however, simultaneously DNA may also condense the packing of the positively charged lipid molecules thus resulting in the condensation of the membrane. Condensation at high pressures is evident for both DPPC/BPDAB and DPPC/HADAB monolayers. The shape of the gel state domains in fluid bulk of DPPC monolayers has been shown to be sensitive to additional compounds included into the film [64–66]. It was recently demonstrated that the cationic surfactant dodecyltrimethylammonium bromide has a pronounced effect on the above domain morphology [67], in accordance with our monolayer results. We could further show that the presence of DNA had a dramatic influence on the domain shapes (Fig. 9B), in keeping with the DSC data revealing DNA to induce phase separation in the binary CL containing alloys.

In brief, these DSC data are compatible with the view that the negatively charged DNA condenses the positively charged lipid headgroups, thus leading to the formation of ordered lipid domains. At a DNA/CL molar ratio > 2.0 the observed broad main transitions with increased enthalpies and the simultaneous disappearance of the DNA-BPDAB transition at higher temperature could be due to DNA-induced vesicle fusion or liposome-induced DNA collapse [23]. A very recent report provides evidence for the entrapment of DNA into the core of the inverted hexagonal phase formed either by proper, H_{II} phase adopting lipids or due to the relief of membrane bending rigidity of the lamellar phase by hexanol [16]. Furthermore, it was demonstrated that, in contrast to the lamellar aggregates, H_{II} phase structures fused and released DNA, when in contact with anionic vesicles, models of cellular membranes. These data are in accordance with the earlier observations that the H_{II} phase forming lipids such as DOPE [46] or DAG [19] promote transfection. It is tempting to speculate that also HADAB could form with DNA H_{II} phase aggregates, in keeping with the pronounced precipitation by DNA of liposomes containing this CL.

Our results show that when complexed with the CLs the thermal denaturation of DNA is prevented. Interestingly, bacteriorhodopsin incorporated into hydrated membranes undergoes denaturation at approximately 90°C. However, when incorporated into dried films the denaturation temperature is increased

to 140°C [68]. Another example is the cytoskeletal protein spectrin [69]. Upon binding to lipid membranes it is protected from thermal denaturation [70]. These results could thus provide a simple mechanistic model for the protection of DNA from thermal denaturation upon complexing with CLs. Upon binding of the protein to a lipid membrane it undergoes a structural transition with the hydrophobic domains becoming incorporated into the interior of the membranes. For spectrin with its pleckstrin homology domain [71], extended lipid anchorage [72] could also be possible. To this end, however, binding of a protein does not per se always mean enhanced resistance to thermal denaturation. A good example is cytochrome *c* for which attachment to liposomes decreases its thermal stability [73]. For DNA, electrostatic interactions play a major role. It has previously been shown that upon binding to lipid membranes DNA undergoes a structural transition [43]. This transition could be caused by the condensation of DNA on the lipid membrane into a stable form, prevented from thermal denaturation.

In conclusion, the differences in the structure of the three CLs, BBDAB, BPDAB and HADAB, with regard to their hydrocarbon chains imposes significantly different physicochemical behaviour to the membranes harbouring these lipids. All these compounds bound DNA and the latter induced phase separation in the binary lipid alloys. The binding of DNA had a dramatic influence on the morphologies of coexisting gel and liquid crystalline domains in monolayers containing CLs. In this regard, monolayers of HADAB were unstabilised by DNA in the subphase, as opposed to BPDAB. This suggests diminished hydrophobicity of HADAB to favour its complex formation with DNA resulting in water soluble complexes. As a further distinction, light scattering measurements revealed DNA–HADAB complexes to be large, which is evident on their precipitation. An important finding is that when complexed with the CLs the thermal denaturation of DNA is prevented.

Acknowledgements

We thank Birgitta Rantala and Riikka Kytömaa for excellent technical assistance. This study was supported by Tekes, Biocentrum Helsinki (P.K.J.K.), Medical Research Council of the Finnish Academy (I.H., P.K.J.K.), The Sigrid Juselius Foundation (I.H.) and The Finnish Cancer Societies (I.H.). J.M.H. is supported by the MD/PhD program of the University of Helsinki and T.P. by the Turku University Graduate School for Medical Sciences.

References

[1] P.L. Felgner, T.R. Gadek, M. Holm, R. Roman, W. Chan, M. Wenz, J.P. Northrop, G.M. Ringold, M. Danielsen, Proc. Natl. Acad. Sci. USA 84 (1987) 7413–7417.
[2] J.G. Smith, R.L. Walzem, J.B. German, Biochim. Biophys. Acta 1154 (1993) 327–340.
[3] A. Singhal, L. Huang, in: J.A. Wolff (Ed.), Gene Therapeutics, Methods and Applications of Direct Gene Transfer, Birkhäuser, Boston, MA, 1994, pp. 118–142.
[4] J.-P. Behr, Bioconjug. Chem. 5 (1994) 382–389.
[5] D.D. Lasic, in: Gene Delivery, CRC Press, Boca Raton, FL, 1997.
[6] J.J. Harrington, G. Van-Bokkelen, R.W. Mays, K. Gustashaw, H.F. Willard, Nature Genet. 15 (1997) 345–355.
[7] W. Roush, Science 276 (1997) 38–39.
[8] P.L. Felgner, G.M. Ringold, Nature 331 (1989) 461–462.
[9] J.H. Felgner, R. Kumar, C.N. Sridhar, C.J. Wheeler, Y.J. Tsai, R. Border, P. Ramsey, M. Martin, P.L. Felgner, J. Biol. Chem. 269 (1994) 2550–2561.
[10] P.L. Felgner, Y.J. Tsai, J.H. Felgner, in: D.D. Lasic, Y. Barenholz (Eds.), Handbook of Nonmedical Applications of Liposomes, Vol. IV, CRC Press, Boca Raton, FL, 1996, pp. 43–56.
[11] J.-Y. Legendre, F.C. Szoka Jr., Pharm. Res. 9 (1992) 1235–1242.
[12] X. Zhou, L. Huang, Biochim. Biophys. Acta 1189 (1994) 195–203.
[13] J. Zabner, A.J. Fasbender, T. Moninger, K.A. Poelinger, M.J. Welsh, J. Biol. Chem. 270 (1995) 18997–19007.
[14] Y. Xu, F.C. Szoka Jr., Biochemistry 35 (1996) 5616–5623.
[15] A.M. Aberle, F. Tablin, J. Zhu, N.J. Walker, D.C. Gruenert, M.H. Nantz, Biochemistry 37 (1998) 6533–6540.
[16] I. Koltover, T. Salditt, J.O. Rädler, C.R. Safinya, Science 281 (1998) 78–81.
[17] D. Harries, S. May, W.M. Gelbart, A. Ben-Shaul, Biophys. J. 75 (1998) 159–173.
[18] P. Harvie, F.M.P. Wong, M.B. Bally, Biophys. J. 75 (1998) 1040–1051.
[19] T. Paukku, S. Lauraeus, I. Huhtaniemi, P.K.J. Kinnunen, Chem. Phys. Lipids 87 (1997) 23–29.
[20] C.H. Spink, J.B. Chaires, J. Am. Chem. Soc. 119 (1997) 10920–10928.
[21] A. Köiv, P. Mustonen, P.K.J. Kinnunen, Chem. Phys. Lipids 70 (1994) 1–10.

[22] A. Köiv, P.K.J. Kinnunen, Chem. Phys. Lipids 72 (1994) 77–86.
[23] H. Gershon, R. Ghirlando, S.B. Guttman, A. Minsky, Biochemistry 32 (1993) 7143–7151.
[24] S.M. Mel'nikov, V.G. Sergeyev, K. Yoshikawa, J. Am. Chem. Soc. 117 (1995) 2401–2408.
[25] S.M. Mel'nikov, V.G. Sergeyev, K. Yoshikawa, J. Am. Chem. Soc. 117 (1995) 9951–9956.
[26] D.L. Reimer, Y. Zhang, S. Kong, J.L. Wheeler, R.W. Graham, M.B. Bally, Biochemistry 34 (1995) 12877–12883.
[27] F.M.P. Wong, D.L. Reimer, M.B. Bally, Biochemistry 35 (1996) 5756–5763.
[28] J.O. Rädler, I. Koltover, T. Salditt, C.R. Safinya, Science 275 (1997) 810–814.
[29] V.A. Bloomfield, Biopolymers 31 (1991) 1471–1481.
[30] M.S. Spector, J.M. Schnur, Science 275 (1997) 791–792.
[31] M. Maccarrone, L. Dini, A. DiGiulio, A. Rossi, M. Giuseppe, A. Finazzi-Agro, Biochem. Biophys. Res. Commun. 186 (1992) 1417–1422.
[32] B. Sternberg, F.L. Sorgi, L. Huang, FEBS Lett. 356 (1994) 361–366.
[33] Y. Fang, J. Yang, J. Phys. Chem. B 101 (1997) 441–449.
[34] Y.S. Tarahovsky, R.S. Khusainova, A.V. Gorelov, T.I. Nicolaeva, A. Deev, A.K. Dawson, G.R. Ivanitsky, FEBS Lett. 390 (1996) 133–136.
[35] N. Dan, Biophys. J. 73 (1997) 1842–1846.
[36] S. May, A. Ben-Shaul, Biophys. J. 73 (1997) 2427–2440.
[37] N. Dan, Biochim. Biophys. Acta 1369 (1998) 34–38.
[38] N.S. Templeton, D.D. Lasic, P.M. Frederik, H.H. Strey, D.D. Roberts, G.N. Pavlakis, Nature Biotechnol. 15 (1997) 647–652.
[39] Y.K. Song, F. Liu, S. Chu, D. Liu, Hum. Gene Ther. 8 (1997) 1585–1594.
[40] J.O. Rädler, I. Koltover, A. Jamieson, T. Salditt, C.R. Safinya, Langmuir 14 (1998) 4272–4283.
[41] Y. Xu, S.W. Hui, P. Frederik, F.C. Szoka Jr., Biophys. J. 77 (1999) 341–353.
[42] S. Huebner, B.J. Battersby, R. Grimm, G. Cevc, Biophys. J. 76 (1999) 3158–3166.
[43] N.J. Zuidam, Y. Barenholz, A. Minsky, FEBS Lett. 457 (1999) 419–422.
[44] T. Akao, T. Fukumoto, H. Ihara, A. Ito, FEBS Lett. 391 (1996) 215–218.
[45] H. Farhood, N. Serbina, L. Huang, Biochim. Biophys. Acta 1235 (1995) 289–295.
[46] L. Wrobel, D. Collins, Biochim. Biophys. Acta 1235 (1995) 296–304.
[47] S.W. Hui, M. Langner, Y.L. Zhao, P. Ross, E. Hurley, K. Chan, Biophys. J. 71 (1996) 590–599.
[48] P.K.J. Kinnunen, Chem. Phys. Lipids 63 (1992) 251–258.
[49] A.L. Bailey, P.R. Cullis, Biochemistry 36 (1997) 1628–1634.
[50] P.K.J. Kinnunen, M. Rytömaa, A. Köiv, J. Lehtonen, P. Mustonen, A. Aro, Chem. Phys. Lipids 66 (1993) 75–85.
[51] A. Köiv, P.K.J. Kinnunen, J. Fluoresc. 4 (1994) 345–347.
[52] A. Köiv, P. Mustonen, P.K.J. Kinnunen, Chem. Phys. Lipids 66 (1993) 123–134.
[53] D.R. Bartlett, J. Biol. Chem. 234 (1959) 466–468.
[54] S. Bhattacharya, M. Subramanian, U.S. Hiremath, Chem. Phys. Lipids 78 (1995) 177–188.
[55] R. Peters, K. Beck, Proc. Natl. Acad. Sci. USA 80 (1983) 7183–7187.
[56] H.M. McConnell, L.K. Tamm, R.M. Weis, Proc. Natl. Acad. Sci. USA 81 (1984) 3249–3253.
[57] I. Solodin, C.S. Brown, M.S. Bruno, C.Y. Chow, E.H. Jang, R.J. Debs, T.D. Heath, Biochemistry 34 (1995) 13537–13544.
[58] S. Mabrey-Gaud, in: C.G. Knight (Ed.), Liposomes: from Physical Structure to Therapeutic Applications, Elsevier/North-Holland Biomedical Press, Amsterdam, 1981, pp. 105–138.
[59] A. Chattopadhyay, E. London, Biochemistry 26 (1987) 39–45.
[60] F.S. Abrams, E. London, Biochemistry 32 (1993) 10826–10831.
[61] D. Hirsch-Lerner, Y. Barenholz, Biochim. Biophys. Acta 1370 (1998) 17–30.
[62] N.J. Zuidam, Y. Barenholz, Biochim. Biophys. Acta 1368 (1998) 115–128.
[63] S.J. Eastman, C.J. Siegel, J. Tousignant, A.E. Smith, S.H. Cheng, R.K. Scheule, Biochim. Biophys. Acta 1325 (1997) 41–62.
[64] R.M. Weis, H.M. McConnell, J. Phys. Chem. 89 (1985) 4453–4459.
[65] H.M. McConnell, D. Keller, H. Gaub, J. Phys. Chem. 90 (1986) 1717–1721.
[66] P.A. Rice, H.M. McConnell, Proc. Natl. Acad. Sci. USA 86 (1989) 6445–6448.
[67] C.W. McConlogue, D. Malamud, T.K. Vanderlick, Biochim. Biophys. Acta 1372 (1998) 24–134.
[68] Y. Shen, C.R. Safinya, K.S. Liang, A.F. Ruppert, K.J. Rothschild, Nature 366 (1993) 48–50.
[69] W. Diakowski, A. Prychidny, M. Swistak, M. Nietubyk, K. Bialkowska, J. Szopa, A.F. Sikorski, Biochem. J. 338 (1999) 83–90.
[70] K. Michalak, M. Bobrowska, A.F. Sikorski, Gen. Physiol. Biophys. 9 (1990) 615–624.
[71] N. Blomberg, M. Nilges, Fold. Des. 2 (1997) 343–355.
[72] P.K.J. Kinnunen, A. Koiv, J.Y. Lehtonen, M. Rytömaa, P. Mustonen, Chem. Phys. Lipids 73 (1994) 181–207.
[73] A. Muga, H.H. Mantsch, W.K. Surewicz, Biochemistry 30 (1991) 7219–7224.